Proceedings of the International Conference on Heat Exchanger Fouling and Cleaning - 2024 (Peer-reviewed)
April 21–26, 2024, Lisbon, Portugal; Editors: H.U. Zettler and E.M. Ishiyama

HOW BIOFILM HISTORY AFFECTS THE IMPACT OF THERMAL DISINFECTION ON BIOFILM CONTROL AND REGROWTH

Ana Rosa Silva[1,2], Luís F. Melo[1,2] and Ana Pereira[1,2*]
[1]LEPABE – Laboratory for Process Engineering, Environment, Biotechnology and Energy, Faculty of Engineering, University of Porto, Rua Dr. Roberto Frias, 4200-465 Porto, Portugal
[2]ALiCE – Associate Laboratory in Chemical Engineering, Faculty of Engineering, University of Porto, Rua Dr. Roberto Frias, 4200-465 Porto, Portugal. * aalex@fe.up.pt

ABSTRACT

Temperature-based strategies are commonly applied to control microbial growth and mitigate the deleterious effect of biofilms on water systems. However, the impact of those thermal procedures on biofilm structure and stability is usually not evaluated. This study addresses specific aspects of the biofilm's structure after being exposed to higher temperatures. Eight days old *Pseudomonas fluorescens* biofilms were formed in a Center for Disease Control (CDC) biofilm reactor under two distinct shear stresses and exposed to 70ºC during 15 min. The biofilm structural features were evaluated 1h and 24 h after disinfection. Biofilm 3D mesoscale structural characteristics have been analyzed through Optical Coherence Tomography (OCT). Biofilms formed under both shear stresses were partially removed after the temperature shock and suffered structural rearrangements over 1h and 24h. Both biofilms seem to rearrange after 24h into structures that combine enhanced compactness with increased porosity. The present work provides a methodology to address future studies concerning the impact of temperature increase on biofilm structural aspects.

Author Keywords. Biofilm, biofilms 3D structure, temperature shock, water systems

INTRODUCTION

Biofilm formation in water networks, and particularly on heat transfer surfaces, has major operational and economical penalties as well as health associated problems. Biofilms are communities of microorganisms organized in a structured system that are enclosed in a self-produced matrix of extracellular polymer substances (EPS). While microorganisms might be directly responsible for corrosion processes, food contaminations or public health issues (like the waterborne pathogen - *Legionella*), the reduction of heat transfer efficiency, the increase of pressure-drop or the equipment failure in water systems are usually a consequence of the impact of the biofilms 3D structure. For illustration purposes, the work from Melo and Flemming (2010) [1] shows that the condensation rate in a condenser might decrease ~30% with the formation of a 100 µm thick biofilm (assuming that the heat transfer coefficient in the condenser is 2500 W/m^{2}K, and that the biofilm thermal conductivity is 0.6 W/mK).

Biofilm structure is vital for the survival and management of the microbial activities within the biofilm. The structure results of the combined effect of hydrodynamics and mass transfer [2], [3], and ultimately affects the biofilm detachment rates [4]. For example, Melo and Vieira [5] showed that *Pseudomonas fluorescens* biofilms formed under lower fluid velocity are more thick and less compact than the ones formed at higher fluid velocities. The later were not so easily detached when subjected to increased shear forces, as the biofilms formed at lower velocities. In water systems, biofilm structure is dynamic and changes over time and space depending on the local specific environmental conditions (hydrodynamics, temperature, pH, nutrients, surface materials, etc). [6].

Minimizing the operational impacts of biofilms is typically accomplished by the implementation of microbiological-control measures, such as thermal disinfection. Thermal disinfection involves increasing of water temperature above the operating temperature of the system, during a certain period of time. It aims to decrease the number of microorganisms in suspension [7], [8]. In water systems like hot water networks, it can be used to reduce the incidence of waterborne pathogens like *Legionella pneumophila* [9]–[12] or *Pseudomonas aeruginosa* [11]–[14]. Or, in the food industry, to control the presence of foodborne pathogens like *Listeria monocytogenes* [15]. Only a few works reported in the literature evaluated the effect of temperature shocks on biofilms.Most of those works tend to be focused on what happens to the microorganisms within the biofilm [16], [17] rather

ISBN: 978-0-9984188-3-4; Published online www.heatexchanger-fouling.com

than what happens to the biofilm in terms of its structure.

The present study investigates how the biofilm mesoscale structure of an 8-day *Pseudomonas fluorescens* biofilm reorganizes itself, 1hour and 24 hours after a temperature shock (70ºC, for 15 min), subject to 125 and 225 RPM rotational speeds. The following biofilm structure parameters have been analyzed: average thickness, porosity and compactness. A first discussion of the effect of the temperature shocks on other microbiological features of the biofilms can be found in Silva et al 2022 [18].

MATERIAL AND METHODS

The present work investigates how 3D biofilm mesoscale properties, especially average thickness, porosity and the compactness, change in relation to hydrodynamics and temperature shocks.

To accomplish the goals of the present study, *Pseudomonas fluorescens* ATCC 13525^T biofilms were grown in a Center for Disease Control (CDC, USA) biofilm reactor for 8 days under two distinct rotational speeds: 125 RPM (shear stress: 0.0205 N/m^2, Re: 1550) and 225 RPM (shear stress: 0.0573 N/m^2, Re: 2800) [19]. These two rotational speeds mimic low flow areas in water systems which might be critical for the development of thicker biofilms and settlement of pathogens like *Legionella pneumophila*.

The CDC Biofilm Reactor is a standardized device commonly used as a drinking water system model to study surface contamination [20]–[23], and it allows biofilm formation under moderate to high fluid shear [24]. It consists of a 1-liter glass beaker with 8 polypropylene rods suspended from a ported lid [24]. Each rod accommodates 3 circular polyvinyl chloride (PVC) coupons with 1.27 cm diameter, that are positioned perpendicularly to a rotating baffle (Fig. 1 – detailed view). PVC was selected as surface material coupons since it is commonly found in drinking water networks where thermal shock are often applied for microbial control [25], [26].

The experimental setup (Fig. 1) consists of the CDC bioreactor placed on top of a magnet stirred plate (in which the stirring velocities are defined), the nutritional medium and waste disposal tank. The bioreactor was filled with 500 mL of nutrient medium [5.5 g/L glucose, 2.5 g/L peptone, 1.25 g/L yeast extract in phosphate buffer (1.88 g/L KH_2PO_4 and 2.6 g/ L $NaHPO_4$] to which 1 mL of an overnight inoculum of ~10^8 CFU/mL *Pseudomonas fluorescens* was added. The bioreactor operated in batch mode for 24h, followed by the continuous addition of nutrient media in a 1:100 ratio at 10 mL/ min, till the end of the experiment.

Biofilms were formed for 8 days (T= 25ºC). By day 8, two holder rods were sampled to characterize the biofilm prior to the T-shock. Bulk water was then replaced by sterile medium (1:100 dilution) at 70ºC (kept constant) and recirculated for 15 min. Several water disinfection procedures at water systems, concerning for example the disinfection of water tanks or mitigation of Legionella pneumophila are accomplished at 70ºC.After that period, the bulk phase was replaced by diluted nutrient media at 25ºC. Biofilms were sampled before and 1h and 24 h after the thermal shock (using the different holders and coupons available). To accomplish the biofilm sampling, a holder rod (3 PVC coupons each) was aseptically removed, and coupons were carefully placed in 12-well microtiter plates filled with 3 mL of a sterile saline solution (8.5 g/L NaCl). Biofilms were imaged using a spectral-domain Optical Coherence Tomography (OCT) - Thorlabs Ganymede Instrument (Thorlabs GmbH, Germany) - with a central wavelength of 930 nm. All volumes are ~2.49×2.13×1.52 mm (y×z×x) and imaged using 509×1024×730 voxels in the corresponding axes. The refractive index was set to 1.40 like the refractive index of water (1.33), as biofilms are mainly composed of water [27].

OCT Images were then analyzed by the freeware software BISCAP (Biofilm Imaging and Structure Classification Automatic Processor) described by Narciso et al. [28] and available at: https://github.com/diogonarciso/BISCAP [28], [29]. Briefly, the pixels in each 2D image at the substratum are identified, a threshold of the pixel's intensity is calculated, and all pixels are binarized according to the biomass or background, allowing to differentiate the full biofilm structure from the liquid bulk phase. The 2D image processing was extended to the 3D OCT images [29]. The final images (as the ones shown in Fig. 2) allows a detailed visualization of the biofilm as each 3D image comprises a set of 509 OCT-2D images. By analyzing those 3D images, the BISCAP delivers a set of parameters commonly used to describe the biofilm structure. In the present work special attention was given to average thickness, porosity and compaction parameter. The average thickness is defined as the total length between the bottom and the top of the biofilm. The compaction parameter, as proposed by Narciso et al. [28], provides a measurement of the biofilm compactness based on the ratio between the continuous biomass pixels in the biofilm structure and the total number of pixels (biomass + water) between the bottom and top interfaces. It ranges between $0<Cp\leq1$, Cp values close to 1 being observed for biofilms with higher compactness (few empty spaces within the biofilm). Finally, porosity is defined as the fraction of background voxels in the biofilm region and changes between 0 and 1 (values close to 0 are observed for biofilms with no porosity).

The experimental data were analysed using the software GraphPad Prism 9.0 for Windows

ISBN: 978-0-9984188-3-4; Published online www.heatexchanger-fouling.com

(GraphPad Software, USA). All measurements were performed in duplicate, and all experiments were performed in three independent replicates. The mean and standard deviation (SD) for each set of results were calculated.

RESULTS AND DISCUSSION

The 8-days *Pseudomonas fluorescens* biofilms, prior to the thermal shock, formed at lower rotational speed (125 RPM) were found to be more heterogenous (Fig. 2 and Fig. 3) and 3.5 times thicker (Fig. 4) than the ones formed at 225 RPM. The biofilms heterogeneity is shown by the profile observed in the topographical figures (Fig. 2). Not surprisingly, the biofilm formed at 125 RPM showed higher porosity and less compactness (lower compaction parameter) than the one at 225 RPM. Several works highlight that biofilms formed under low shear forces tend to be very heterogenous, and to have pores and protuberances [30]. These differences in the biofilm's structures reflect the impact of the hydrodynamic conditions, particularly the fluid shear forces on the coupons which are known to affect mass transfer and erosion (removal) across the biofilm surface [30]–[32]. Increasing the fluid velocity, increases the turbulence near the surface, which favors the rate of mass transfer from the bulk phase to and from the biofilm, enhancing the exchange of nutrients, oxygen, metabolic waste (among others). However, simultaneously the biofilm is subjected to higher shear forces, thus increasing the removal rate and decreasing the biofilm thickness.

After biofilms exposure to 70ºC for 15 min, biofilms exhibit different structural properties depending on the hydrodynamic conditions. Concerning the biofilm formed at 125 RPM, the T-shock had a significant effect on average thickness reduction, which decreased from 132 µm (before the T-shock) to 43 µm (1h after the T-shock), indicating a significant biofilm sloughing-off. Consequently, the biofilm became more homogenous, as can be seen in Fig. 2 (2^{nd} row). Simultaneously, these biofilms became slightly more compact (~0.65) – Fig. 6 - in response to the T-shock (or because of the biofilm removal), yet the porosity (~0.26) remained constant (Fig. 5).

On the other hand, biofilms grown under 225 RPM did not show significant changes in terms of average thickness (Fig. 4) which remained the same before and after the thermal shock (~ 41 µm), suggesting that biofilm sloughing-off was not significant. A detailed analysis of the topographical images shows that there is a greater heterogeneity on this biofilm after being exposed to the temperature increase. The maximum thickness (red color in Fig. 2, d) found before, and 1h after the T-shock is respectively, 152 µm and 425 µm. The 425 µm thickness is expectedly due to parts of the biofilm that detached from the surface in one point but are still connected to the surface on the other extremity. This aspect is clear when comparing the 2D images selected from the 3D images stacks (Fig. 3 a) and c)) that have similar maximum biofilm thicknesses. It is not surprising that the 225 RPM can sustain such a thick biofilm not fully supported at the surface, as the adhesion and cohesion forces of biofilms formed at higher shear stresses are higher than for lower shear stresses [33]. The existence of a significant sloughing-off for the 225 RPM condition is further confirmed by the surface area coverage reduction determined via Confocal Laser Scanning Microscopy in a complementary study [18]. It is widely reported that biofilms formed under higher shear stress conditions tend to more resistant to external stresses like biocides, flow changes (etc.) [34], [35], but grounding sloughing off conclusions solely on the average thickness, as represented in Fig. 4, can be misleading. At 225 RPM, the other structural parameters significantly changed before and 1h after the T-shock: compactness (Fig. 6) decreased from 0.88 to 0.55 and porosity (Fig. 5) increased from 0.11 to 0.28.

Biofilm thermal resistance is proportional to the biofilm thickness [2] and is also dependent on the hydrodynamics conditions: as fluid velocities increase the fouling thermal resistance decreases [2]. Given that at lower fluid velocity (125 RPM) the biofilms were initially thicker - both aspects (hydrodynamics and thickness) contribute to the thermal resistance increase. As so, the heat transfer rate along the biofilm (from the top to the surface) will be lower at 125 RPM than at 225 RPM. Thus, it might be feasible to accept that after 15 min, the temperature profile along the biofilm will be different for the two evaluated conditions. Probably this justifies why there were no significant differences on porosity and compaction parameter for the 125 RPM biofilms before and after the T-shock, yet those were very significant for the 225 RPM. Additionally, Pavlovsky et al. [36] showed that the mechanical properties of *Staphylococcus epidermidis* biofilms changed when exposed to 60ºC during 1h. The authors hypothesized that temperature weakened the mechanical integrity of the biofilm matrix, even though no significant effect was found regarding the chemical EPS constituents. Another important aspect that might be considered is the effect of temperature on the viscoelasticity of the biofilms. Viscoelasticity is known to be an essential feature underlying biofilms protection to chemical and physical stresses [37]. Mechanical stresses might lead to cohesive failure (when the detachment forces acting in the biofilm exceed the forces between the different organisms in the biofilm) and/or adhesive failure (when the detachment forces action in the biofilm exceed the forces of adhesion to the surface – biofilm dislodgement).

ISBN: 978-0-9984188-3-4; Published online www.heatexchanger-fouling.com

The 1h after-the-shock data seem to represent a transient effect of the 70ºC on the biofilm at the same conditions under which it was formed (25ºC). The 24h data represents a more stable condition of the structural rearrangements of the biofilms. Analyzing the biofilm structural parameters 24h after the thermal shock shows that, regardless the rotational speed considered (125 or 225 RPM), the biofilms reached similar average thicknesses (Fig. 4) ~ 64.7 µm, and compaction parameters (Fig. 6) ~ 0.80. It is worth to note that the 125 RPM biofilm, like what was observed before the shock, is more heterogenous than the 225 RPM one (higher shear stress).

The present study only considered the mesoscale structural aspects of the biofilms, ignoring for example microbiological aspects. Yet, from the perspective of the biofilm's history, after being subjected to an external stressors, it is expected that it rearranges into a more 'robust' structure that becomes better prepared for future external impacts [18]. As so, it is not surprising that, even keeping the same balance between mass transfer and shear forces as in the initial biofilm, the 125 RPM matrix rearranges into a thinner and more compact biofilm. On the other hand, the 225 RPM biofilm seems to have made a trade-off between keeping its compactness and increasing porosity (the 225 RPM biofilm before the T-shock has reduced porosity). The water-filled areas withing the biofilm (direct contributors to the porosity) have very important functional characteristics for the bacteria survival and biofilm preservation, like for example to transport nutrients, waste-products (etc) or to store key components to cells [38], and was suggested that water inside biofilms (in pores or in water-channels) can be seen as a human rudimentary vascular system [38]. In this assumption, it is not surprising that after a shock the balance between porosity and compactness is duly considered by the microbial films. Furthermore, the rapid regrowth and rearrangement of the biofilms after 24h is an important argument supporting the implementation and proper monitoring of temperature-based microbiological control approaches [7].

Further research is needed to explore the mechanisms behind structural rearrangements in response to thermal shocks. The compactness of the biofilm layers, as well as their susceptibility to sloughing-off, are critical to heat exchanger thermal performance, pressure drop across water systems and to health prevention in the case for example of *Legionella* control in cooling water systems or in hot water networks. It might be also important to understand how the thermal shock affect biofilm recalcitrance, stability and resilience upon new mechanical stresses (temperature, flow shifts, etc).

Figures

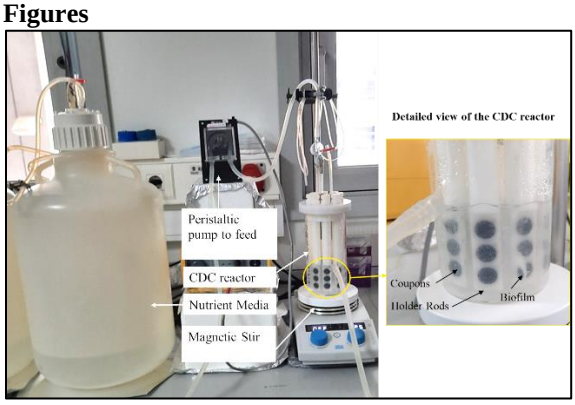

Fig. 1 Photography of the experimental setup. A detailed view of the CDC reactor is provided on the right.

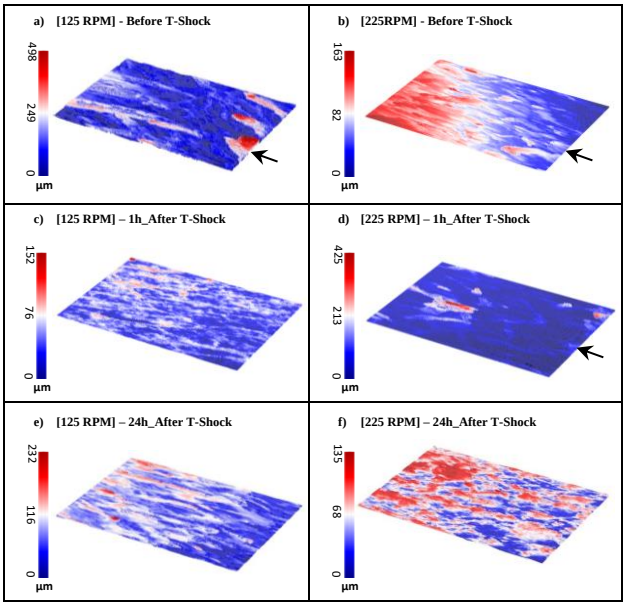

Fig. 2 *Pseudomonas fluorescens* biofilms 3D-topographical view, prior the temperature shock (T-Shock) and 1h and 24h after the Temperature shock. Each image is the reconstruction of 509 images 2D-OCT stacks. In brackets the rotation speed imposed during biofilm formation and T-shock. Image colors: red corresponds to the maximum thickness of the biofilm; black to the lowest biofilm areas (0 µm).

ISBN: 978-0-9984188-3-4; Published online www.heatexchanger-fouling.com

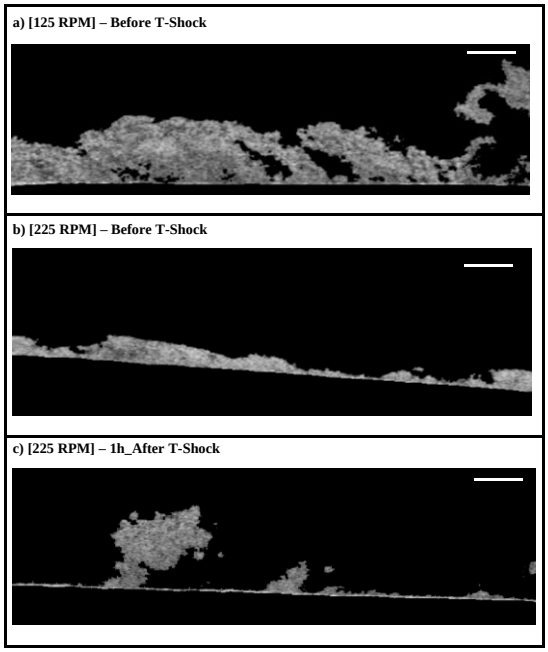

Fig. 3 OCT 2D images selected from the 3D image stack corresponding to the topographical views in Fig. 2, at the position marked with an arrow. Only the representative conditions of 125 RPM_before T-Shock, 225 RPM_before T-shock, 225 RPM_1h after T-shock. The scale bar corresponds to 100 µm.

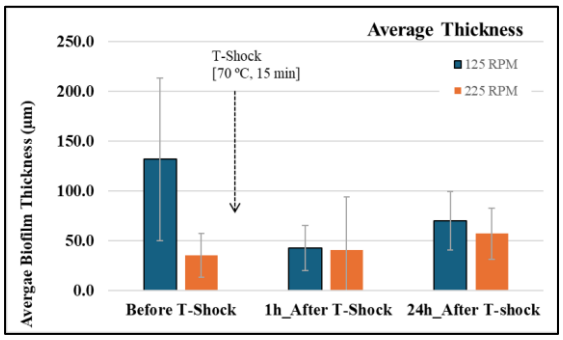

Fig. 4 Biofilm average thickness calculated from the 3D biofilm images represented in Fig. 2. The error bars correspond to the standard deviation.

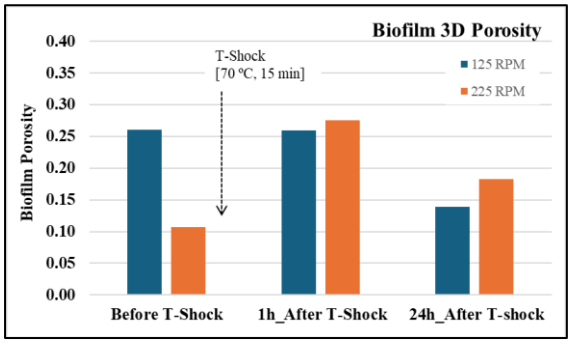

Fig. 5 Biofilms porosity before and 1h and 24h after the temperature shock (T-shock) for the tested rotational velocities 125 RPM and 225 RPM. Data corresponds to the biofilms depicted in Fig. 2.

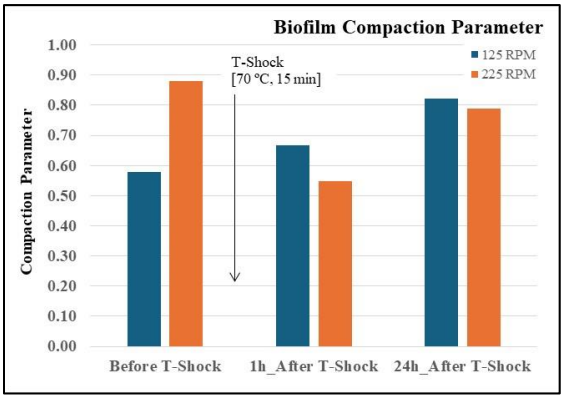

Fig. 6 Biofilms compaction parameter before and 1h and 24h after the temperature shock (T-shock) for the tested rotational velocities 125 RPM (blue bars) and 225 RPM (orange bars). Data corresponds to the biofilms depicted in Fig. 2.

Copyright permissions. All images are original. No copyright permissions are required.

CONCLUSION

The present work provides a preliminary study about the impact of temperature shock on biofilms mesoscale structure. It also establishes a methodological approach that can, in future works, address specific aspects of the impact heat transfer on the biofilm structure to design better adjusted thermal procedures and minimize the operational penalties of biofilms.

The main conclusions point out that the thermal shocks effects depend on the hydrodynamic conditions, particularly 1 h after the shock. The biofilms regrow and rearrange rapidly and 24h after the thermal shock both structures seem to reach a trade-off between porosity and compactness, reaching similar values.

NOMENCLATURE

Re Reynolds number, dimensionless
T Temperature, °C
RPM Rotation per min, RPM

ACKNOWLEDGMENTS

This work was supported by national funds through FCT/MCTES (PIDDAC): LEPABE, UIDB/00511/2020 (DOI: 10.54499/UIDB/00511/2020) and UIDP/00511/2020 (DOI: 10.54499/UIDP/00511/2020) and ALiCE, LA/P/0045/2020 (DOI: 10.54499/LA/P/0045/2020). And under the project 2022.03523.PTDC - LegioFilms - Understanding

ISBN: 978-0-9984188-3-4; Published online www.heatexchanger-fouling.com

the Role of Biofilm Architecture in Legionella Colonization and Risk of Detachment in hospital networks using an Integrated Monitoring Approach, with DOI 10.54499/2022.03523.PTDC (https://doi.org/10.54499/2022.03523.PTDC). Ana Rosa Silva thanks the Portuguese Foundation for Science and Technology (FCT) for the financial support of the PhD grant (2020.08539.BD).

REFERENCES

[1] Melo, L., and Flemming, H.-C., Mechanistic Aspects of Heat Exchanger and Membrane Biofouling and Prevention, in *The Science and Technology of Industrial Water Treatment*, ed. Z. Amjad, pp. 365–380, Taylor & Francis, Boca Raton (USA), 2010.

[2] Vieira, M., Melo, L., and Pinheiro, M., Biofilm formation: Hydrodynamic effects on internal diffusion and structure, *Biofouling*, vol. 7, no. 1, pp. 67–80, 1993.

[3] Lewandowski, Z., and Beyenal, H., *Fundamentals of Biofilm Research*, 2nd ed. CRC Press, Boca Raton, 2013.

[4] Stoodley, P., Lewandowski, Z., Boyle, J. D., and Lappin-Scott, H. M., Structural deformation of bacterial biofilms caused by short-term fluctuations in fluid shear: an in situ investigation of biofilm rheology, *Biotechnology and Bioengineering*, vol. 65, no. 1, pp. 83–92, 1999.

[5] Melo, L. F., and Vieira, M. J., Physical stability and biological activity of biofilms under turbulent flow and low substrate concentration, *Bioprocess Engineering*, vol. 20, no. 4, pp. 363–368, 1999.

[6] Donlan, R. M., Biofilms: microbial life on surfaces, *Emerging Infectious Disease*, vol. 8, no. 9, pp. 881–890, 2002.

[7] Nocker, A, Lindfeld, E., Wingender, J., Schulte, S., Dumm, M., and Bendinger, B., Thermal and chemical disinfection of water and biofilms: only a temporary effect in regard to the autochthonous bacteria, *Journal of Water and Health*, vol. 19, no. 5, pp. 808–822, 2021.

[8] Cebrián, G., Condón, S., and Mañas, P., Physiology of the Inactivation of Vegetative Bacteria by Thermal Treatments: Mode of Action, Influence of Environmental Factors and Inactivation Kinetics, *Foods*, vol. 6, no. 12, pp. 1-12, 2017.

[9] Mouchtouri, V., Velonakis, E., and Hadjichristodoulou, C., Thermal disinfection of hotels, hospitals, and athletic venues hot water distribution systems contaminated by *Legionella* species, *American Journal of Infection Control*, vol. 35, no. 9, pp. 623–627, 2007.

[10] Blanc, D. S., Carrara, P, Zanetti, G., and Francioli, P., Water disinfection with ozone, copper and silver ions, and temperature increase to control *Legionella*: seven years of experience in a university teaching hospital, *Journal of Hospital Infection*, vol. 60, no. 1, pp. 69–72, 2005.

[11] Yui, S., Karia, K., Ali, S., Muzslay, M., and Wilson, P., Thermal disinfection at suboptimal temperature of *Pseudomonas aeruginosa* biofilm on copper pipe and shower hose materials, *Journal of Hospital Infection*, vol. 117, pp. 103–110, 2021.

[12] Zhang, C., Qin, K., Struewing, I., Buse, H., Domingo, J. S., Lytle, D., and Lu, J., The Bacterial Community Diversity of Bathroom Hot Tap Water Was Significantly Lower Than That of Cold Tap and Shower Water, *Frontiers in Microbiology*, vol. 12, pp. 1-21, 2021.

[13] Ricker, E. B., Aljaafari, H. A. S., Bader, T. M., Hundley, B. S., and Nuxoll, E., Thermal shock susceptibility and regrowth of *Pseudomonas aeruginosa* biofilms, *International Journal of Hyperthermia*, vol. 34, no. 2, pp. 168–176, 2018.

[14] Ricker, E. B., and Nuxoll, E., Synergistic effects of heat and antibiotics on *Pseudomonas aeruginosa* biofilms, *Biofouling*, vol. 33, no. 10, pp. 855–866, 2017.

[15] Tsai, H. -C., Taylor, M. H., Song, X., Sheng, L., Tang, J., and Zhu, M. -J., Thermal resistance of *Listeria monocytogenes* in natural unsweetened cocoa powder under different water activity, *Food Control*, vol. 102, pp. 22–28, 2019.

[16] Farhat, M., Trouilhé, M. C., Briand, E., Moletta-Denat, M., Robine, E., and Frère, J., Development of a pilot-scale 1 for *Legionella* elimination in biofilm in hot water network: Heat shock treatment evaluation, *Journal of Applied Microbiology*, vol. 108, no. 3, pp. 1073–1082, 2010.

[17] Wahlen, L., Parker, A., Walker, D., Pasmore, M., and Sturman, P., Predictive modeling for hot water inactivation of planktonic and biofilm-associated *Sphingomonas parapaucimobilis* to support hot water sanitization programs, *Biofouling*, vol. 32, no. 7, pp. 751–761, 2016.

[18] Silva, A. R., Narciso, D. A. C., Gomes, L. C., Martins, F. G., Melo, L. F., and Pereira, A., Proof-of-concept approach to assess the

ISBN: 978-0-9984188-3-4; Published online www.heatexchanger-fouling.com

impact of thermal disinfection on biofilm structure in hot water networks, *Journal of Water Process Engineering*, vol. 53, pp. 103595, 2023.

[19] Goeres, D. M., Loetterle, L. R., Hamilton, M. A., Murga, R., Kirby, D. W., and Donlan, R. M., Statistical assessment of a laboratory method for growing biofilms, *Microbiology*, vol. 151, no. 3, pp. 757–762, 2005.

[20] Armbruster, C. R., Forster, T. S., Donlan, R. M., O'Connell, H. A., Shams, A. M., and Williams, M. M., A biofilm model developed to investigate survival and disinfection of *Mycobacterium mucogenicum* in potable water, *Biofouling*, vol. 28, no. 10, pp. 1129–1139, 2012.

[21] Lu, J., Buse, H. Y., Gomez-Alvarez, V., Struewing, I., Santo Domingo, J., and Ashbolt, N. J., Impact of drinking water conditions and copper materials on downstream biofilm microbial communities and *Legionella pneumophila* colonization, *Journal of Applied Microbiology*, vol. 117, no. 3, pp. 905–918, 2014.

[22] Szwetkowski, K. J., and Falkinham, J. O., *Methylobacterium* spp. as Emerging Opportunistic Premise Plumbing Pathogens, *Pathogens*, vol. 9, no. 2. pp. 1–9, 2020.

[23] Spencer, M. S., Cullom, A. C., Rhoads, W. J., Pruden, A., and Edwards, M. A., Replicable simulation of distal hot water premise plumbing using convectively-mixed pipe reactors, *PLoS One*, vol. 15, no. 9, pp. e0238385, 2020.

[24] Johnson, E., Petersen, T., and Goeres, D. M., Characterizing the Shearing Stresses within the CDC Biofilm Reactor Using Computational Fluid Dynamics, *Microorganisms*, vol. 9, no. 8, pp. 1709, 2021.

[25] McBain, A. J., Bartolo, R. G., Catrenich, C. E., Charbonneau, D., Ledder, R. G., Rickard, A. H., Symmons, S. A., and Gilbert, P., Microbial Characterization of Biofilms in Domestic Drains and the Establishment of Stable Biofilm Microcosms, *Applied and Environmental Microbiology*, vol. 69, no. 1, pp. 177–185, 2003.

[26] Morvay, A. A., Decun, M., Scurtu, M., Sala, C., Morar, A., and Sarandan, M., Biofilm formation on materials commonly used in household drinking water systems, *Water Supply*, vol. 11, no. 2, pp. 252–257, 2011.

[27] Romeu, M. J., Alves, P., Morais, J., Miranda, J. M., Jong, E. D., Sjollema, J., Ramos, V., Vasconcelos, V., and Mergulhão, F. J. M., Biofilm formation behaviour of marine filamentous cyanobacterial strains in controlled hydrodynamic conditions, *Environmental Microbiology*, vol. 21, no. 11, pp. 4411–4424, 2019.

[28] Narciso, D. A. C., Pereira, A., Dias, N. O., Melo, L. F., and Martins, F. G., Characterization of biofilm structure and properties via processing of 2D optical coherence tomography images in BISCAP, *Bioinformatics*, vol. 38, no. 6, pp. 1708-1715, 2022.

[29] Narciso, D. A. C., Pereira, A., Dias, N. O., Monteiro, M., Melo, L. F., and Martins, F. G., 3D optical coherence tomography image processing in BISCAP: characterization of biofilm structure and properties, *Bioinformatics*, 2024.

[30] van Loosdrecht, M. C. M., Eikelboom, D., Gjaltema, A., Mulder, A., Tijhuis, L., and Heijnen, J. J., Biofilm structures, *Water Science and Technology*, vol. 32, no. 8, pp. 35–43, 1995.

[31] Tsagkari, E., and Sloan, W. T., Turbulence accelerates the growth of drinking water biofilms, *Bioprocess and Biosystems Engineering*, vol. 41, no. 6, pp. 757–770, 2018.

[32] Soares, A., Gomes, L. C., Monteiro, G. A., and Mergulhão, F. J., Hydrodynamic Effects on Biofilm Development and Recombinant Protein Expression, *Microorganisms*, vol. 10, no. 5. pp. 1–10, 2022.

[33] Pereira, M., Kuehn, M., Wuertz, S., Neu, T., and Melo, L. F., Effect of flow regime on the architecture of a *Pseudomonas fluorescens* biofilm., *Biotechnology and Bioengineering.*, vol. 78, no. 2, pp. 164–171, 2002.

[34] Simões, L. C., Gomes, I. B., Sousa, H., Borges, A., and Simões, M., Biofilm formation under high shear stress increases resilience to chemical and mechanical challenges, *Biofouling*, vol. 38, no. 1, pp. 1–12, 2022.

[35] Cunault, C., Faille, C., Calabozo-Delgado, A., and Benezech, T., Structure and resistance to mechanical stress and enzymatic cleaning of *Pseudomonas fluorescens* biofilms formed in fresh-cut ready to eat washing tanks., *Journal of Food Engineering*, vol. 262, no. 6, pp. 154–161, 2019.

[36] Pavlovsky, L., Sturtevant, R. A., Younger, J. G., and Solomon, M. J., Effects of temperature on the morphological, polymeric, and mechanical properties of

ISBN: 978-0-9984188-3-4; Published online www.heatexchanger-fouling.com

Staphylococcus epidermidis bacterial biofilms, *Langmuir*, vol. 31, no. 6, pp. 2036–2042, 2015.

[37] Peterson, B. W., He, Y., Ren, Y., Zerdoum, A., Libera, M. R., Sharma, P. K., van Winkelhoff, A. -J., Neut, D., Stoodley, P., van der Mei, H. C., and Busscher, H. J., Viscoelasticity of biofilms and their recalcitrance to mechanical and chemical challenges, *FEMS Microbiology Reviews*, vol. 39, no. 2, pp. 234–245, 2015.

[38] Quan, K., J. Hou, Zhang, Z., Ren, Y., Peterson, B. W., Flemming, H. -C., Mayer, C., Busscher, H. J., and van der Mei, H. C., Water in bacterial biofilms: pores and channels, storage and transport functions, *Critical Reiews in Microbiology.*, vol. 48, no. 3, pp. 283–302, 2022.

ISBN: 978-0-9984188-3-4; Published online www.heatexchanger-fouling.com